Journal of Materials Chemistry B

Paper

Designing Polymeric Adhesives for Antimicrobial Materials: Poly(ethylene imine) Polymer, Graphene, Graphene Oxide and Molybdenum Trioxide - A biomimetic Approach

Received 00th January 20xx,
Accepted 00th January 20xx

DOI: 10.1039/x0xx00000x

www.rsc.org/

Hang N. Nguyen[a], Enrico T. Nadres[a], Bryan G. Alamani[b], Debora F. Rodrigues[a*]

The synthesis of biocompatible polymers for coating applications has been gaining more attention in recent years due to increasing spread of infectious diseases via contaminated surfaces. One strategy to combat this problem is to apply antimicrobial coatings to surfaces prone to microbial contamination. This study presents a series of biomimetic polymers that can be used as adhesives to immobilize known antimicrobials agents on surfaces as coatings. Several polymers containing dopamine methacrylate as co-polymers were synthesized, and investigated as adhesives for the deposition of an antimicrobial polymer (polyethyleneimine) and antimicrobial nanoparticles (graphene, graphene oxide and molybdenum trioxide) onto glass surfaces. The results showed that different anti-microbials required different types of adhesives for effective coating. Overall, the coatings fabricated from these composites were shown to inactivate *E. coli* and *B. subtilis* within 1 hr. These coatings were also effective to prevented biofilm growth and were demonstrated to be non-toxic to human corneal epithelial cell line (htCEpi). Leaching tests of coatings proved that the coatings are stable under biological conditions.

Introduction

The strong adhesive properties of the sticky byssus of the freshwater zebra mussels have inspired many researchers to synthesize catechol-containing adhesive bio-polymers, such as poly[(dopamine methacryalamide)-*stat*-(2-methoxy acrylate)-*stat*-(ethylene glycol dimethacrylate), which is known to be as strong as commercial preparations of Krazy Glue® and Epoxy®.[1, 2, 3] These bio-inspired polymers are also known to exhibit excellent adhesiveness to a variety of surfaces, ranging from smooth organic surfaces of polytetrafluoroethylene (PTFE) to roughened inorganic surfaces.[4] Like the byssus proteins, the effectiveness of these other bioinspired catechol-containing polymers are mainly due to the binding properties of the catechol groups.[5]

Previous studies using simple polymerization of dopamine at basic pH showed that these adhesives can be useful in many medical applications, such as soft tissue attachment and bone repair.[6] The major drawbacks of using only poly-dopamine and most of the current bioinspired adhesive polymers are twofold: first, these current polymers do not present anti-microbial properties and therefore can be a source of nosocomial infections, which affect per year 2 million people and add more than $5 billion in medical costs. Second, the incorporation of anti-microbial components in these polymers is very difficult due to specific pH and solvent requirements. For instance, the occurrence of polymerization of dopamine occurs in aqueous solutions, which would prevent easy synthesis of composites with anti-microbial properties that require organic solvents.

Our strategy was to synthesize polymeric adhesives whose design was based on the catechol-rich proteins of mussel byssus. Since the catechol side chains of the proteins are responsible for the adhesive properties of the mussel byssus, the incorporation of monomers with catechol side chains in the newly designed polymers resulted into adhesive polymers with similar adhesive property to the mussel byssus. The adhesive polymer, in turn was used to bind surfaces and different anti-microbial materials together to generate an antimicrobial surface.

[a] Department of Civil and Environmental Engineering, University of Houston, Houston, TX 77204 – 4003 (U.S.A.)
*Corresponding Author's Email: dfrigirodrigues@uh.edu Phone: +1-713-743-1495
[b] Department of Chemical Engineering, University of the Philippines, Diliman, Quezon City, Philippines 1101

† Electronic Supplementary Information (ESI) available: [details of any supplementary information available should be included here]. See DOI: 10.1039/x0xx00000x

The antimicrobials selected for this investigation were the synthetic polyethyleneimine polymer (PEI) and nanoparticles of graphene (G), graphene oxide (GO) and molybdenum trioxide (MoO_3). These antimicrobials were selected for this study because they have very distinct properties, compositions, origins, and have been demonstrated to possess strong antimicrobial properties.[7-10] Furthermore, these antimicrobials are either soluble or can be easily suspended in water, hence their coatings are not very stable for long time, unless they are "glued" to the surfaces. The main scientific question was whether an adhesive material would work with different types of anti-microbials.

One of the materials evaluated was PEI, which was chosen to represent soluble polymers with antimicrobial properties. PEI belongs to a class of cationic polymers that interacts with the negatively charged components of cell membranes and eventually destroying them.[11] In addition to PEI, two types of nanoparticles (metal oxide and carbon nanomaterials) were used to investigate the nanoparticle interactions with the bio-inspired adhesive polymers. The rationale for selecting these nanomaterials was because they have been previously described to be potent antimicrobials against antibiotic resistant microorganisms, including Methicillin-resistant *Staphylococcus aureus* (MRSA). In the past years, polymer nanocomposites have also been showing promise as safer anti-microbial agents as opposed to their pristine counterparts.[12-14, 15, 16] For instance, nanocomposites of GO and G showed superior antimicrobial properties then their pure counterparts as well as negligible mammalian cytotoxicity.[13, 14, 17]

The MoO_3 nanoparticles, on the other hand, were selected as representatives of emerging metal oxide antimicrobials. MoO_3, has not been extensively investigated as silver, titanium oxide and other metal-based nanoparticles and hence its antimicrobial properties is still poorly understood. MoO_3 has also been shown to be activated under visible light and present two main types of crystal morphologies.[18] The MoO_3 crystal forms, *h* and α-MoO_3, have recently been described to exhibit antimicrobial properties against pathogenic microbes.[19] In these studies, *h*-MoO_3 was shown more active in terms of oxygen species production under visible light and to have anti-microbial properties against *E. coli*, *K. pneumoniae*, *S. aureus*, and *P. aeruginosa.*[8, 20, 21]

In this study, we synthesized four different types of polymer adhesives that contain catechol groups mimicking the adhesiveness of the mussel adhesive proteins. The synthetic adhesive polymers were then used to deposit anti-microbial polymers (PEI) or nanoparticles (G, GO and MoO3) onto surfaces. Our strategy differs significantly from the accepted standard coating procedures since current deposition techniques rely mostly on activation of either the surface or material to be deposited. In our strategy, modification of the surface or antimicrobial material is not necessary, since the antimicrobial materials can be used directly without any chemical derivatization or functionalization. Upon mixing the nanomaterials with the polymers, the resulting composite can be coated onto diverse surfaces directly. This strategy greatly simplifies the deposition of soluble or suspendible materials. With this strategy, we aim to produce antimicrobial coatings consisting of polymer composites, graphene-based polymer nanocomposites, as well as a new type of metal oxide nanoparticle (MoO_3) polymer nanocomposite with antimicrobial properties, but safe for humans. The antimicrobial composites coatings were characterized and investigated for initial cell attachment, anti-biofilm activity and human cytotoxicity. The stability of the coatings was also investigated using leaching assays.

Experimental Methods

Nanoparticles and polyethyleneimine

Graphene (G) was purchased from XG science and the characterization can be found in our previous study.[22] The modified Hummer's method was used to synthesize graphene oxide (GO) from the graphite. The molybdenum trioxide (*h*-MoO_3) was synthesized according to a previous described method, which involves the precipitation of acidified ammonium molybdate solution.[21] The X-ray diffraction (XRD), Fourier Transform Infrared Spectroscopy (FTIR), Raman Spectroscopy and X-ray photoelectron spectroscopy (XPS) and Scanning electron microscope (SEM) characterizations of GO and *h*-MoO_3 can be found in the supporting information (Fig. S1 and S2).

Dopamine methacrylamide (DMA). The 3-hydroxytyramine HCl (42 mmol, 8 g) was mixed with 75 mL of anhydrous methanol in a nitrogen-purged 250 ml round bottom flask with a magnetic stir bar. Triethylamine (43.2 mmol, 6.0 mL) was then added and the solution was stirred at 0 °C. Methacryloyl chloride (5.85 mmol, 6.0 mL) was then injected in the flask. Another portion of triethylamine (43.2 mmol, 6.0 mL) was added. The solution was stirred under room temperature for 16 h. The product was isolated by removing most of the methanol with a rotavap. The thick residue was extracted with ethyl acetate (3 X 100 mL). The organic layers were combined and washed with HCl solution (1N, 3 X 100 mL), followed by washing with saturated sodium chloride (100 mL) and then dried with magnesium sulfate. The filtered solution was concentrated to about 100 mL and the solution was stored in freezer overnight to precipitate the DMA product. The white crystal products were filtered, washed with cold ethyl acetate and dried. The identity of the product was confirmed by proton NMR analysis. ^{1}H NMR (DMSO-d6, 400 MHz) δ 8.7–8.6 (2H), 7.9 (1H), 6.5–6.6 (2H), 6.42 (1H), 5.61 (1H), 5.30 (1H), 3.21 (2H), 2.55 (2H), 1.84 (3H).

Synthesis of adhesive polymers

The synthesis of the adhesives was done via free radical polymerization of DMA with other monomers.[23] The other monomers used were 2-methoxyethyl acrylate (polymer A), no copolymer (polymer B), ethyl methacrylate (polymer C), and 2-hydroxyethyl methacrylate (polymer D). Typically, a 1.5 mmol of DMA (1.5 mmol, 332 mg), 8.5 mmol of the other monomer (either A, C or D) and 2,2'-azobisisobutyronitrile (AIBN, 1.0 mmol, 164 mg) were dissolved in dimethylformamide (DMF, 5 mL). The solution was bubbled with N_2 for 5 min and heated at 60 °C for 16 h. The product was isolated by addition of methylene chloride to the cooled reaction mixture, followed by dropwise addition of the resulting mixture to hexane (200 mL)

to induce precipitation of the polymer. The polymer precipitate was obtained after centrifugation (5000 rpm, 10 min). The precipitate was dissolved in dichloromethane (5 mL) and reprecipitated in hexane. The polymer precipitation was done twice. Finally, the polymers were dried under vacuum. The molecular weight of the polymers was determined using gel permeation chromatography and the confirmation of the structure was done using nuclear magnetic resonance. Please see details below for the synthetic procedure for polymers A–D.

Polymer A. Poly(DMA-co-MEA). DMA (1.5 mmol, 332 mg), 2-methoxyethyl acrylate (MEA, 8.5 mmol, 1.10 mL), (AIBN, 1.0 mmol, 164 mg) and DMF (5 mL) were mixed in a vial with septum, degassed and mixed at 60 °C for 16 h. After purification, the yield was 1.03 g. The polymer was analysed by NMR. ^{1}NMR ($CDCl_3$, 500 MHz) δ 6.85–6.43 (m), 4.18 (br s), 3.55 (br s), 3.34 (br s), 2.79–2.53 (m), 2.45–2.16 (m), 2.08 (br s), 1.91 (br s), 1.79–1.22 (m), 1.09–0.78 (m).

Polymer B. Poly-DMA. DMA (5.0 mmol, 1.10 g), AIBN (0.5 mmol, 82 mg) and DMF (2.5 mL) were mixed in a vial with septum were mixed in a vial with septum, degassed and mixed at 60 °C for 16 h. The polymer product was isolated by the addition of dichloromethane (2.5 mL) to the cooled reaction mixture followed by adding the resulting solution drop wise to excess hexane (100 mL). After purification, the yield was 1.30 g. The structure of the polymer was confirmed by NMR analysis. ^{1}H NMR (DMSO-D6, 500 MHz) δ 8.83–8.50 (m), 7.35 (br s), 6.68–6.24 (m), 3.05 (br s), 2.44–2.40 (m), 1.73–1.26 (m), 1.05–0.88 (m).

Polymer C. Poly-(EMA-co-DMA). DMA (1.5 mmol, 332 mg), ethyl methacrylate (EMA, 8.5 mmol, 1.06 mL, AIBN (1.0 mmol, 164 mg) and DMF (5 mL) were mixed in a vial with septum, degassed and mixed at 60 °C for 16 h. After purification, the yield was 1.20 g. The structure of the polymer was confirmed by NMR analysis. ^{1}H NMR ($CDCl_3$, 500 MHz) δ 6.95–6.51 (m), 4.03 (br s), 3.44 (br s), 2.69 (br s), 2.18–1.65 (m), 1.16–0.79 (m).

Polymer D. Poly-(HEMA-co-DMA). DMA (1.5 mmol, 332 mg), 2-hydroxyethyl methacrylate (HEMA, 8.5 mmol, 1.03 mL), AIBN (1.0 mmol, 164 mg) and DMF (5 mL) were mixed in a vial with septum. The mixture was bubbled with nitrogen for 5 min and then stirred at 60 °C overnight, degassed and mixed at 60 °C for 16 h. The polymer product was isolated by adding methanol (2 mL) to the cooled reaction mixture followed by dropwise addition of the resulting mixture to excess diethyl ether (200 mL). The collected polymers were dried under vacuum (yield, 1.20 g). ^{1}NMR (DMSO-d6, 500 MHz) δ 8.78–8.54 (m), 7.71–7.36 (m), 6.66–6.28 (m), 4.79 (br s), 3.86 (br s), 3.03 (br s), 2.44–2.43 (m), 2.08–1.50 (m), 1.02–0.8 (m).

Fabrication of the coated slides

Stocks of 1000 ppm of adhesive polymer (polymers A–D) solutions were prepared by dissolving the polymers in solvents (methanol for polymer A, DMF for polymers B–D), followed by sonication for 10 min. In another set of vials, 1000 ppm mixture of antimicrobial agents (PEI, graphene and graphene oxide and *h*-MoO_3) were prepared by suspending in solvents (methanol for PEI, DMF for *h*-MoO_3, graphene and graphene oxide) followed by sonication for 30 min. For each adhesive polymer solution, different proportions (25, 50, 75, 85 %) of each antimicrobial agents (*i.e.* PEI, GO, G and MoO_3) were added to give an adhesive concentration of 250, 500 and 750 ppm, respectively. The resulting mixtures were sonicated further for 10 min prior to application as coatings.

Small pieces of glass slides (1.0 cm X 2.5 cm) were cleaned by sonicating in 2-propanol followed by rinsing with deionized water and dried at 105°C. The glass slides were cooled and loaded into the spin coater. The prepared mixtures were dropped in the centre of the glass slide and the spin coater was started (initial spin 30 rpm, 10 s; final spin, 3000 rpm, 50 s). The coatings on the glass slides were then annealed in the oven at 70 °C for 16 h. The coated glass slides were characterized and assayed for anti-microbial activity. The best antimicrobial results obtained for each type of antimicrobial adhesive nanocomposite were selected for further investigation.

Characterizations of the coatings on glass slide

The characterizations of the coatings were carried on with the samples resulting in higher antimicrobial properties (see results below). The static sessile drop contact angle of water in uncoated and coated glass slides were determined.[24] Briefly, a droplet on the surface was generated with a syringe held vertically to the surface. A high resolution camera was used to capture the images of the droplets followed by analysis with ImageJ.[25] All the measurement was done in triplicate for triplicate samples and the average and standard deviations were calculated. Scanning Electron Microscopy (SEM, Leo 1525 Gemini Zeiss) was used to take the images of the nanoparticles on coated surfaces. The other characterizations (FTIR and XPS) of the coatings can be found in supporting information.

Leaching test of the adhesive coatings

These experiments were performed to show that the coatings are stable and not leaching any toxic components to the test solutions. Uncoated and coated glass slides were placed in 6-well plates containing 5 mL of sterile phosphate buffered saline solution (PBS, pH = 7.4, Sigma Aldrich, U.S.A.). The plate was incubated for 7 d at 37°C. Then, the PBS solution was withdrawn from the wells and tested for *E. coli* toxicity. Briefly, in a 2 mL Eppendorf, 900 µL of the PBS leachate and 100 µL of *E. coli* suspension (0.2 of OD_{600}) were mixed and incubated at 35°C for 2 h. Serial dilutions were performed after the incubation period and the microorganisms were plated on tryptic soy agar plate (TSA, Oxoid, U.S.A.) in triplicate. The plates were incubated at 35°C for 12 h and the colony forming units (CFU/mL) were determined. After the leaching test, the coated slides were characterized again using FTIR (PEI coating), XPS (PEI and MoO_3 coatings), and SEM (MoO_3, G and GO coatings) to confirm the coatings were still intact. Ellipsometry was also used to determine any changes in thickness of the coatings after the leaching test.

Bacterial suspension preparation

Antimicrobial experiments were carried out using Gram-negative (*Escherichia coli* MG 1655) and Gram-positive (*Bacillus subtilis* 102) microorganisms. A 16 h culture was freshly prepared each time in tryptic soy broth (TSB, Oxoid, U.S.A.). All

the growth was conducted at 35 °C while shaking at 150 rpm (ThermoFisher, U.S.A). To harvest the cells, the growth medium was centrifuged at 10,000 rpm for 5 min, and then rinsed twice using PBS, thereby completely removing the TSB media. The bacterial pellet was then re-suspended in PBS at 0.05 optical density of 600nm (OD_{600}), which corresponds to 5 x 10^4 CFU/mL.

Live/dead assay

Each coated slide was rinsed with PBS and 70% ethanol following by air-drying under the sterile biosafety hood before placing at the bottom of sterile 6-well plates (BioLite, U.S.A.). Control samples, such as the uncoated glass slides and slides coated only with the adhesive polymers investigated, followed the same procedure as the investigated samples. An aliquot of 4 mL bacterial suspension was added to each well to fully cover the coated slides, and then the plate was incubated at 35°C for 1h and 2h without shaking. After the incubation period, the slides were removed using a sterile tweezer. The LIVE/DEAD Baclight bacterial viability kit (Invitrogen, U.S.A), which contains SYTO9 and propidium iodide (PI) dyes, was used to investigate for membrane disruption caused by the antimicrobial coatings. The staining procedure was explained in our previous study.[26] The fluorescent images at 40x objective were taken using Olympus microscope (BX 51 Olympus Fluorescent Microscope) equipped with DP72 digital camera and Fluorescein isothiocyanate (FITC) filter. All the experiments were performed in triplicate. The results were calculated from the Eq. 1, and then the averages and standard deviations were obtained. The *t*-test was used to determine statistically significance of the results.

$$\text{Dead cells (\%)} = \frac{\text{Number of dead cells (Red)}}{\text{Number of total cells (Green)}} \text{ x } 100 \qquad \text{(Eq. 1)}$$

Scanning Electron Microscopy (SEM) images

SEM images of *B. subtilis* and *E. coli* were obtained on the surface of uncoated and coated slides. The same procedure as the Live/dead assay with a 2 h incubation time was followed to obtain the cell initial attachment to the surfaces. After incubation, the slides were removed with sterile tweezers to proceed to the fixation immediately. A 200 µL solution of 2% glutaraldehyde in 0.05 M Cacodylate buffer was added to completely cover the slide surface. The details of the fixation, post-fixation with 1% osmium tetraoxide and washing can be found in our previous study.[27] Finally, the slides were coated with gold at 0.05 Torr, 40 mAmps in 40s (Denton V Desk Sputter). The images were acquired using a scanning electron microscope (SEM Leo 1525 Gemini Zeiss).

Biofilm assay: crystal violet and confocal images

The composite containing PEI was coated directly on the bottom of the wells of 96-well plate by adding 100 µL of the solution (C-PEI75) prepared earlier, followed by drying and annealing at 70 °C. Wells coated with polymer C only was also prepared. Prior to adding the bacteria to the coated 96-well plate, they were grown in TSB for 16 h at 35°C. The growth cultures were diluted at ratio 1:100 using the growth medium. The detail procedure of the biofilm formation quantification was described in previous studies.[28, 29] Briefly, the final biofilm was measured through the crystal violet absorption method using a microplate reader at 540 nm wavelength (Biotek Synergy, U.S.A.). The results were averaged out and standard deviations were also obtained. Since the nanocomposites containing G (B-G50), GO (D-GO75) and MoO_3 (A-$MoO_3$50) were suspended in DMF, direct coating of the bottom of the well was not possible since the plates are made of plastic. Therefore, crystal violet assay was not performed for these samples. Instead, biofilm formation was further investigated by obtaining confocal microscopy images of the biofilm grown on coated glass slides with the adhesives. The bacterial cultures were prepared similarly to the crystal violet assay described above. Coated and uncoated glass slides were placed in 6-well plates and 100 µL of the diluted bacterial suspension and 6 mL of growth medium was added to each well. All the plates were incubated at 35 °C for 72 h. The z-stack images of the biofilms were acquired using Leica Confocal (10x/0.3 HCPL FLUOTAR, LEICA TCS SPE). The images were analysed using Comstat 2.1.2 to obtain the biomass and maximum thickness.[30-32] Six images were taken for each sample and the experiments were done in triplicate. The results were averaged for all results and standard deviations were also obtained.

Cytotoxicity of the coatings against human corneal epithelial cell

The human cytotoxicity was performed using the PBS solution after the leaching experiment as previously described.[27] The CellTiter 96 Aqueous One Solution Cell Proliferation Assay kit (Promega, USA) and immortalized human corneal epithelial cell line (hTCEpi) in KBM-2 complete media (Lonza, U.S.A Catalog# CC-3107) were used in this experiment to investigate the safety of PBS solution that was in contact with the coated glass slides. Briefly, hTCEpi cells with density of 30 x 10^4 cells per mL were prepared from a 48 h culture flask (passage number 48). Then, aliquots of cell suspension (100 µL) were added to the wells containing 100 µL of test solutions: PBS from leaching experiment, negative control (sterile PBS) or positive control (0.02% of benzalkonium chloride, BAC). At the same time, the wells with KBM medium without cells were prepared for each sample to subtract the background. The plates were incubated at 37 °C with 5% CO_2 humidified incubator (NuAire, U.S.A) for 24 h. All the samples were prepared in triplicate. After 24 h, the wells were washed three times with sterile PBS. The CellTiter reagent and KBM were added to the wells and then incubated for another 3 h before reading the fluorescence at 490 nm (FLUOstar Omega, BMG Labtech, Germany). The percentages of living cells were then calculated. The results were averaged and standard deviations were also obtained.

The growth of hTCEpi cell line on the surface of glass slides coated with adhesive and PEI or nanoparticles (G, GO and *h*-MoO_3) were also investigated. In this experiment, the Live/Dead Cell Imaging kit (R37601, Invitrogen, U.S.A) was employed to determine any damage to the cells in contact with the coated surfaces. A concentration of 30 x 10^4 of hTCEpi cells per mL was prepared as described above. The coated slides and a negative control (glass slide only) were placed in a sterile 6-well plate.

Then, 3 mL of cell suspension was introduced and the cell culture was incubated at 37 °C for 16 h. After 16h, the slides were removed from the wells using a sterile tweezer; and then, a 10 µL of dye was added over the slides and incubated at room temperature for 5 min. The staining dye mixture was prepared following the manufacture's protocol.[33] The fluorescent images were taken using confocal microscopy (10x/0.3 HCPL FLUOTAR, LEICA TCS SPE). Additionally, the images were also taken using the Olympus microscope (BX 51 Olympus Fluorescent Microscope) for viable cell counts. A positive control was also prepared from the uncoated glass slides after 16 h cell incubation. This positive control followed a treatment with 0.02% BAC for 15 min before the staining process. The experiment was performed in replicate and six images were taken for each sample and control. The results were expressed in term of percentage of dead cells which were obtained using Equation 2.

$$\text{Dead cells (\%)} = \frac{\text{Number of dead cells (Red)}}{\text{Number of total cells (Green+red)}} \text{ x } 100 \qquad \text{(Eq. 2)}$$

Ellman's assay for detection of reactive oxygen species (ROS)

In the Ellman's assay, the ROS activity was quantified indirectly through the loss of glutathione (GSH) activity.[34, 35] The uncoated slide (control) and coated slides with adhesive A, B, C, D, A-$MoO_3$50 (50% of MoO_3), B-G50 (50% of G), C-PEI75 (75% of PEI) and D-GO75 (75% of GO) were placed in 15 mL conical tubes containing 2 mL of 0.4 mM GSH (dissolved in 50 mM bicarbonate buffer, pH 8.6) and 2 mL of $NaHCO_3$. A positive control containing 2 mL of 30% H_2O_2 was prepared in parallel and treated with the same reagents. The samples were left shaking at 150 rpm for 2 h at room temperature. After that, 500 µL of samples were withdrawn and placed in 2 mL tubes. The samples were analysed as described previously.[35] The absorbance was read at 412 nm (Synergy MX Microtiter plate reader, BioTek, U.S.A.) and the results were express in terms of loss of GSH which was calculated from equation 3.

$$\text{Loss of GSH (\%)} = \frac{\text{(absorbance of negative control} - \text{absorbance of sample)}}{\text{absorbance of negative sample}} \text{ x } 100 \qquad \text{(Eq. 3)}$$

Results and Discussions

Synthesis and Characterization of the polymers.

This study aims to design adhesive polymers that will simultaneously immobilize and promote the natural antimicrobial properties of a polymer (PEI) and nanoparticles (*h*-MoO3, graphene and graphene oxide). The adhesive polymers that were prepared have catechol side chains and a co-polymer that provide side groups with a variety of properties. A 15 % amount of catechol groups was chosen to approximate the amount found in naturally occurring mussel adhesion proteins,[36] as well as in many previously described synthetic polymer adhesives.[37] The different side groups, on the other hand, were investigated for effective interaction of the antimicrobials with the adhesive polymers. Scheme 1 shows the synthetic reaction and the variation of side chains that has been incorporated in the synthesized adhesive polymers. Polymer A contained a polar aprotic side chain, Polymer B is composed of only a monomer with a catechol side chain (homopolymer), polymer C contained a short hydrophobic side chain, and polymer D contained a polar protic hydroxyl side chain. NMR analysis of the obtained

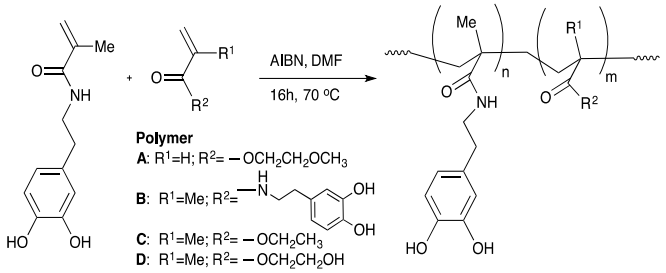

Scheme 1: Synthesis of polymeric adhesives

Table 1: Table of NMR/GPC for **c**haracterization of the adhesives polymer used in this study

Polymer	MP_n (NMR)[a] Mol %	M_n (GPC)[b] g/mol	M_w (GPC)[b] g/mol	Đ[c]
A	84	27 509	39 527	1.44
B	0	7 554	15061	1.99
C	84	4 136	7 710	1.86
D	85	29 525	44 691	1.51

[a] Mole percent of copolymer (MP_n) in a polymer chain determimed by ^{1}H NMR.
[b] The number average molecular weight (M_n), The weight average molecular weight (M_w) determimed by GPC. The molecular weight calibration was based on polystyrene standards.

polymers proved that the proportion of the catechol side chain of the polymers was around 15 %. The proportion of the catechol was determined by comparing the integrated area of the methylene groups of DMA and co-polymers. (NMR Spectra is presented in the *Supporting information*). GPC analyses estimated that the polymers have low molecular weight of 7-45 kDa (Table 1). The slight differences in sizes of the polymers should have little effect on our application since they will be cross-linked into 3-D networks when applied as coatings. Also, GPC estimated the polydispersity index to be between 1.4-2.0, values that are commonly observed for polymers of this type prepared by free radical polymerization. [37, 38]

Selection of the best polymer.

There was a total of four synthesized polymers that were evaluated as adhesives for coatings with antimicrobial materials onto glass surfaces. Experiments were performed to determine which polymers were the best adhesives for each type of antimicrobial material. In this initial assessment, mixtures of the adhesive polymers with PEI, G, GO or *h*-MoO_3 with 50:50 (wt/wt) ratio were first prepared and used to coat glass slides by spin coating. *E. coli* culture was then exposed to the coated surfaces and the bacterial mortality was assessed using the live and dead assay. At a 50:50 ratio of adhesive polymers and antimicrobials materials, all of the combinations coated on the glass slides exhibited antimicrobial properties. These results

show the adhesive polymers did not hinder the antimicrobial properties of the materials tested. The percentage of inactivated cells ranged between 20 and 80% (Fig. 1).

The antimicrobial activity was further investigated by varying the ratio of adhesive polymer and antimicrobial agents. Results for the incorporation of PEI to adhesive polymers showed that PEI's combination with polymer C exhibited the highest antimicrobial activity (Fig. 1). This observed result is consistent with other studies that suggested that the presence of a hydrophobic side chain, such as the one found in Polymer C, enhanced the antimicrobial activities of amine-based polymers. The presence of cationic and hydrophobic regions in the polymers were shown to provide more effective and synergistic interactions between the polymers and microbial membranes.[39-41] The cationic part of the coating provides the initial electrostatic attraction to the negatively charged components of the cells such as phosphate group of lipids, while the hydrophobic part interacts with the hydrophobic region of the lipid bilayer, eventually destroying it.[42]

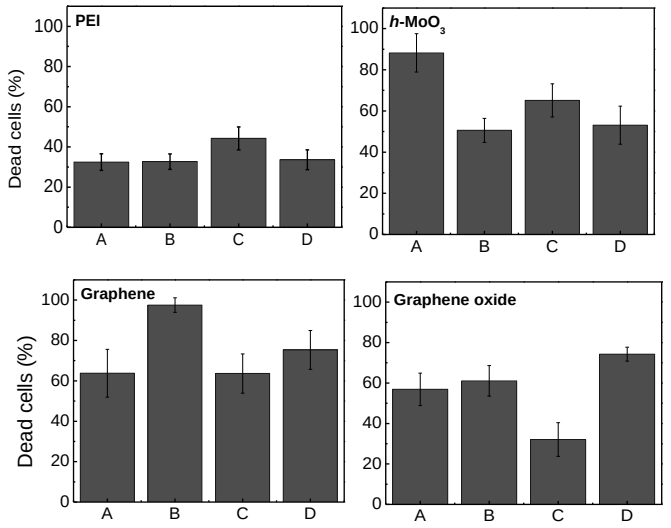

Fig.1. Live and Dead assessment to select the best adhesives (A, B, C, D) for each antimicrobial material. Results are expressed as percentage of dead cells (coatings with 50% adhesive and 50% materials exposed for 2 h to the cells). The controls: glass slides only and adhesives only did not show any dead cells (not presented in the figures).

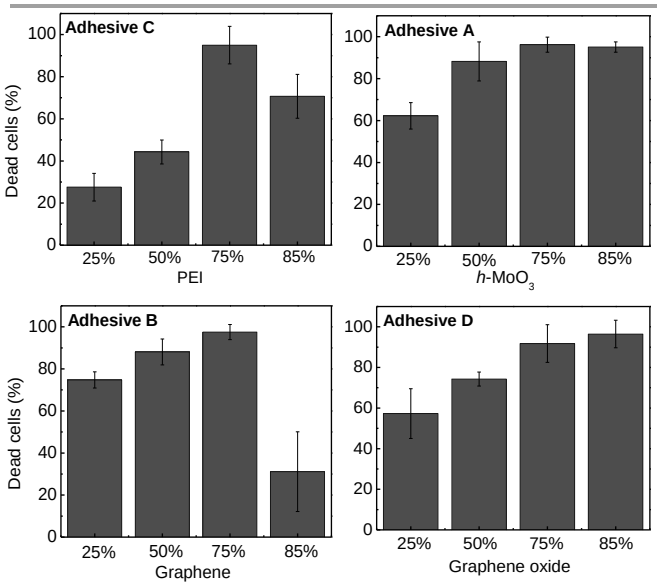

Fig. 2. Selection of the best ratio of antimicrobials with their respective adhesives. The results using live and dead assay are expressed as percentage of dead cells (2 h exposure). The controls: glass slides only and adhesives only did not present any dead cells (data is not presented in the figures). The coatings contained 25, 50, 75 and 85% of antimicrobial materials.

Among the different ratios of Polymer C with PEI, the best antimicrobial property was observed on a mixture containing 25% of polymer C and 75% of PEI (C-PEI75), which resulted into 95 ± 8.9% dead cells (Fig 2). Similar increase in antimicrobial activity towards *E. coli* and *S. aureus* was observed on soluble cationic polymers upon addition of co-polymer with hydrophobic side chains at more than 20% mol fraction.[43] Addition of more PEI in the mixture (85 %) did not increase the antimicrobial activity, presumably because polymer C was already saturated.

In the case of nanoparticles, different kinds of adhesive polymers were found to be optimum for each of them. For the two carbon-based nanoparticles, polymer B and D worked the best for graphene and graphene oxide, respectively (Fig. 1). Graphene is non-polar and has aromatic rings in its structures, which facilitate π-bond interactions. Therefore, the π-π bonding between the catechol rings of polymer B with that of graphene sheets generated a better antimicrobial coating. Antimicrobial assays of coatings made from different percentages (25, 50, 75 and 85%) of adhesives showed that the coatings composed of 50:50 combination of polymer B and graphene (B-G50) had the best performance (Fig. 2). Note, that the addition of more graphene did not increase the antimicrobial activity. Others working with graphene and polymer composites also observed that graphene's performance as an antimicrobial material was enhanced due to increase dispersion of this nanomaterial in the polymer.[14, 44] Hence, higher concentrations of graphene will lead to higher aggregation and reduced antimicrobial property.

Meanwhile, the polymer D adhesive with more polar side chains, such as hydroxyl groups, was a more effective adhesive for GO because of the hydrogen bonding. Further assays showed that the ratio of 25% of polymer E with 75% GO (D-GO75) exhibited the best antimicrobial effect (Fig. 2).

In the case of molybdenum trioxide (*h*-MoO_3), a metal oxide nanoparticle, incorporated better in the polymer A, which contains an ether group as side chain (Fig. 1). Further experiments showed that at 50% *h*-MoO_3 (A-$MoO_3$50), the antimicrobial property reached close to 100% (Fig. 2).

Characterizations of the best coatings for each antimicrobial

Homogeneity of the coatings

SEM images of glass slides coated with polymer A, B, and D were found to be smooth and uniform (Fig. 3). SEM images of the surface deposited with A-$MoO_3$50, B-G50, and E-GO50 showed nanoparticles homogenously deposited on the surface. The nanoparticles were randomly distributed on the surface.

In contrast to the nanoparticles, the coatings of polymer C and the composite C-75PEI also presented smooth surfaces. The nature of the PEI (not a particle) did not allow the visualization of the polymer on the surface. Therefore, the characterization of polymer C and C-75PEI coatings was carried out with XPS (Fig. 4) and additional FTIR characterization of C-75PEI can be found in the *Supporting Information.* Analyses of the coated samples

showed carbon, oxygen and nitrogen content, which correspond to the atoms of the adhesive polymer backbone (polymer C). In comparison to polymer C, the polymer C and PEI composite showed higher proportion of nitrogen. Deconvolution of the peaks showed increased proportion of the C–N bond and decreased proportion of the C–O bond. These results demonstrate the formation of crosslinked bonds between the adhesive polymer and PEI.

Change of contact angle of coated glass slides

The successful coatings were monitored by determining changes on the surface property of the coated glass slides through contact angle measurements. The results showed that the starting uncoated glass slides were very hydrophilic (17.5°). Upon coating with the adhesive polymers, hydrophobicity of the surface increased (Fig. 5). For example, the contact angle of the glass slide coated with polymer C increased to 69.7°. This is due to the hydrophobic ethyl group side chain component of the polymer. Addition of hydrophilic PEI polymer to the adhesive polymer C (C-PEI75) resulted in lower contact angle (57.1°) compared to the surface coated with the Polymer C only. In the case of polymer B, the change in contact angle of the glass slide was marginal, but increased substantially when coated with B-G50. Clearly, the hydrophobic nature of graphene[45] has imparted its properties to the nanocomposite product. On the other hand, the presence of polar polymer D coating has increased the contact angle (39.1°) of the glass surface and addition of GO to the polar adhesive (D-GO75) increased the contact angle only a little bit more (43.2°). And lastly, coating the glass slide with polymer A and the corresponding composite with *h*-MoO_3 (A-$MoO_3$50) exhibited water contact angle of 55.1° and 58.6°, respectively. These significant increases in contact angle showed further proof of successful coating of the glass slides with the prepared adhesive polymers and composites.

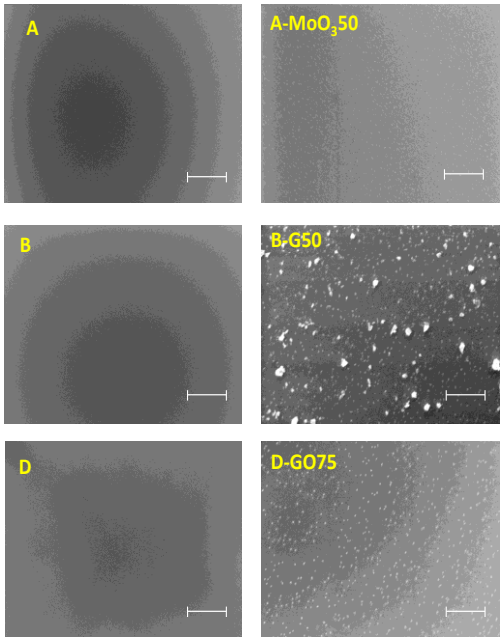

Fig. 3. Scanning electron microscope (SEM) images of the coatings: polymer A, A-$MoO_3$50, polymer B, B-G50, polymer D and D-GO75 showing the nanoparticles on the surface of the coatings. Scale bar 1µm.

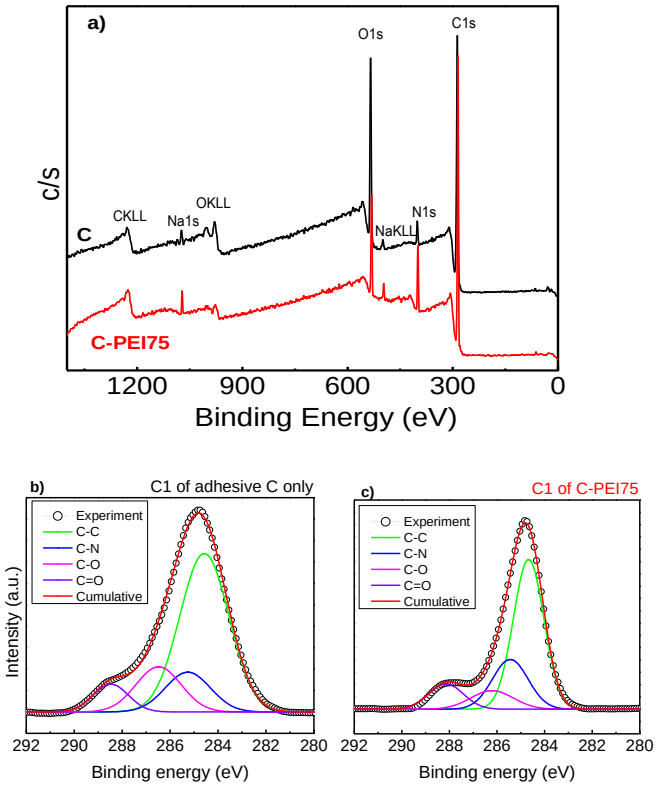

Fig. 4: XPS spectra of the coatings: adhesive C only and C-PEI75 (adhesive C with 75% PEI) showing the increase in nitrogen on the coated surface indicating the presence of PEI and adhesive (a). The C1s of high resolution of C (b) and C-PEI75 (c) were also expressed in the figures with more C-N bonding in the carbon bonding of the coatings with PEI.

Stability of the coatings through leaching test

This experiment was performed to test for the potential release of coating materials in solution. The solution used for leaching (7 d) was tested for toxicity against bacteria and human cells. Results showed that there was no sign of toxicity to either bacteria or human cells after incubation for 2 h and 16 h, respectively (Fig. 6 and 7). The nontoxic results of the leaching solution confirmed that there was no significant release of coating materials to aqueous solutions.

To confirm the stability of the coatings, the glass slides were re-characterized after the leaching tests to determine any surface changes. The C-PEI75 coatings were characterized using FTIR and XPS, which showed similar spectral characteristics as the coating prior to the leaching assay (See *Supporting Information*, Fig. S4a and S4b). Similarly, B-G50, D-GO75 and A-$MoO_3$50, were also re-characterized after the leaching test (Fig. S4c and S5). The thickness of the coatings was also evaluated before and after leaching for 7 days at 37 ^{0}C. The results showed no significant losses of the coating (See *Supporting Information*, Table S1). These results indicate that the polymeric adhesives can produce stable coatings under biological conditions.

Antimicrobial effects and human toxicity of the coatings

Antimicrobial effects: concentrations, time dependency and morphological changes

From the results, other important trends were observed. First, the optimum concentration of polymers C and B as adhesive

coatings can only be as low as 25% because the antimicrobial activity declines when lower concentrations are used (Fig. 2). In contrast, polymers A and D could be used with a concentration as low as 15% and still present excellent antimicrobial activities. The hydrogen bonding interaction of the polymers with the nanomaterials could have played a key role in creating a more effective bond between the materials and the adhesives. Furthermore, PEI and GO exhibited a concentration dependency. For instance, microbial inactivation was 74 ± 3.5% and 92 ± 9.2% with PEI concentrations of 50% and 75%, respectively. In the case of GO, at 50% and 75%, the microbial inactivation was 44 ± 5.7% and 95 ± 8.9%, respectively (Fig. 2). This similar trend in concentration dependency was previously reported for GO and PEI.[10, 35, 46] However, this trend was not observed for G and *h*-MoO_3, in which the antimicrobial activities showed a plateau and were not significantly different at concentrations above 50% for graphene and 25% for *h*-MoO_3 (Fig. 2). These results contradict previously reported antimicrobial studies that showed concentration dependency for these nanoparticles. [14, 47] In the present case, addition of more graphene and *h*-MoO_3 (≥ 50%) did not improve the antimicrobial activity, presumably because the aggregation of particles cancelled the addition effect of more antimicrobial material.

After the ratio selection of adhesives and antimicrobials was completed, further investigation was carried out against different Gram-negative and Gram-positive bacteria to determine the range of anti-microbial activity of the coatings.

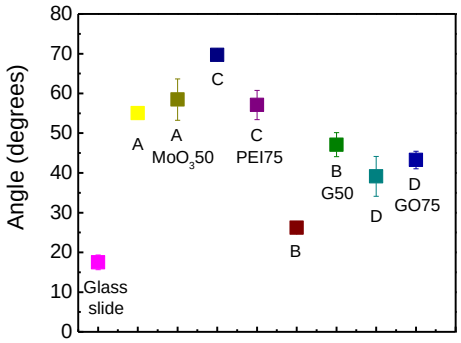

Fig. 5: Contact angle results of the best coatings. The coatings presented are the adhesives and antimicrobial materials, namely: adhesive C with 75% PEI (C-PEI75), adhesive A with MoO_3 50% (A-$MoO_3$50), adhesive B with graphene 50% (B-G50) and adhesive D with graphene oxide 75% (D-GO75).

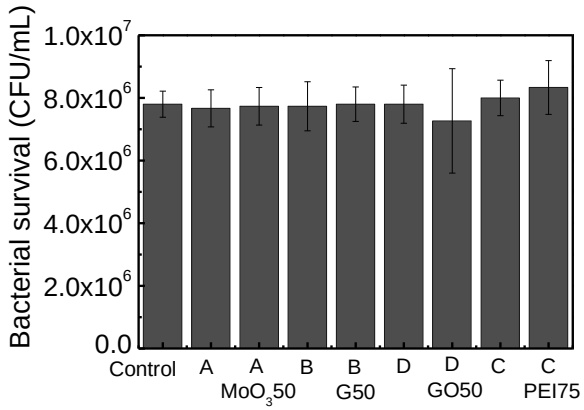

Fig. 6: Investigation of bacterial survival after contact with leaching solutions. *E. coli* K12 was exposed to the solutions that were in contact with the coatings for 7d. The microbial survival was determined using the plate count method.

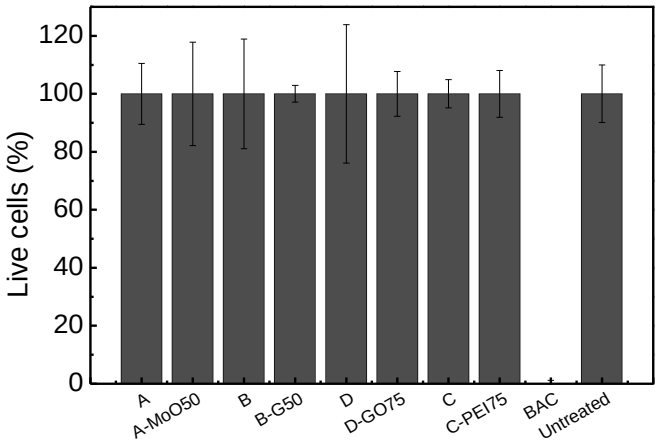

Fig. 7: Cytotoxicity of leaching solution against hTCEpi cell line (human corneal epithelial). The solution was exposed for 24h to the coatings prior to exposure to the cell line. The negative control with untreated cells and positive control using benzalkonium chloride (BAC) 0.02% are also presented in the figure. The standard deviations are presented as error bars.

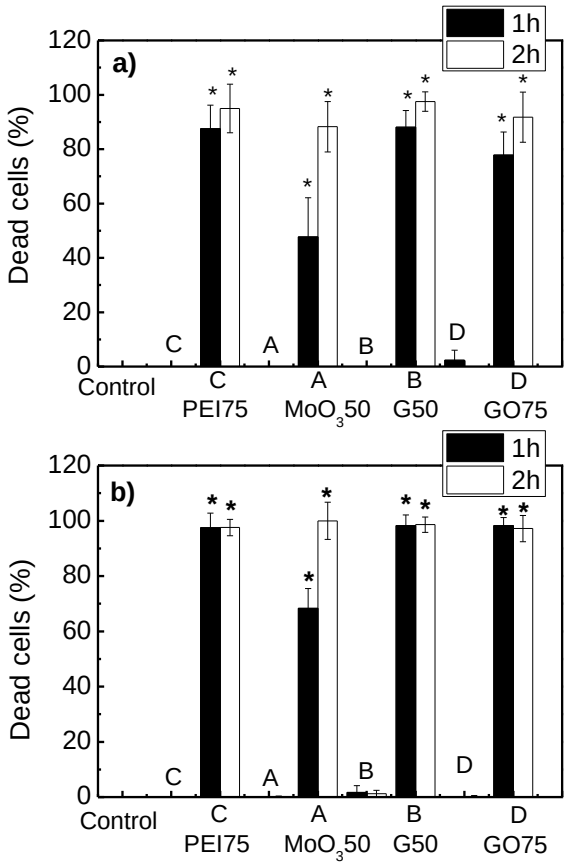

Fig. 8: Live and dead assays of the coatings expressed as percentage of dead cells of *E. coli* (a) and *B. subtilis* (b). The results represent the microbial inactivation after 1 and 2 h interactions between microorganisms and coated surfaces. The controls consisted of only glass slides and the adhesives on the slide. The controls presented a result of zero or less than 2% of dead cells. The symbol (*) indicates statistically significant results between the control (slides coated with the adhesive only) and the adhesive composites.

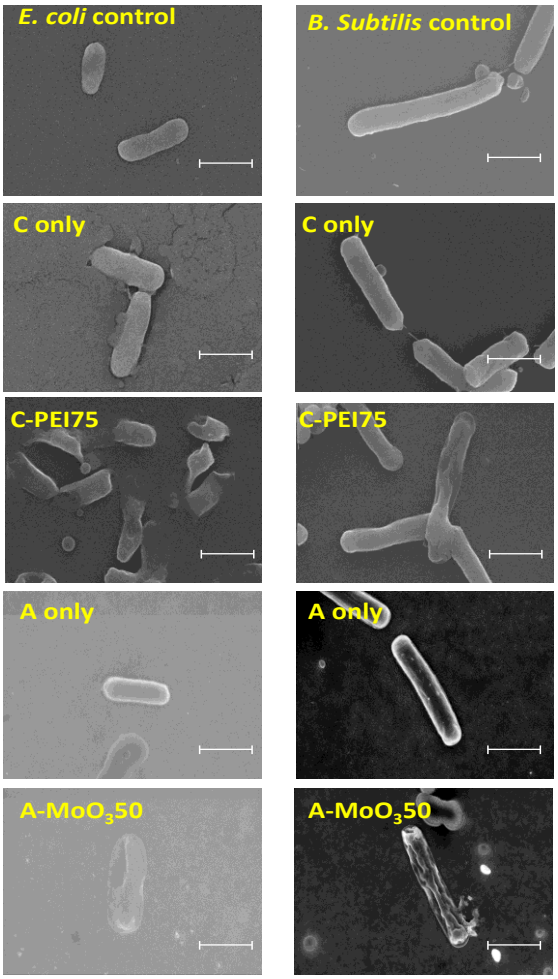

Fig. 9: Scanning Electron Microscope (SEM) images showing the damaged microbial cells after interacting with the coating surface for 2h. In this experiment *E. coli* and *B.* subtilis cells were used. Scale bar at 1 µm.

The toxicity of the slides coated with composites exhibited excellent activity against *E. coli* after 1 h interaction (from 78 to 98% of dead cells) for most coatings, except for A-$MoO_3$50 (48%). While uncoated glass slides and slides coated with adhesives showed no dead cells (Fig. 8a). Also, the results demonstrated that the polymer adhesives enhanced the antimicrobial activity of graphene and GO due to more efficient contact between the coated surface and bacteria. [14, 26] The antimicrobial assays also revealed that compared to *E. coli* samples, *B. subtilis* had more cells inactivated after 1 h interaction for all antimicrobials.

The experiments also revealed that the antimicrobial activity of the coatings C-PEI75, B-G50 and D-GO75 took a little longer to inactivate *E. coli* than *B. subtilis. B. subtilis f*or these coatings was inactivated in less than 1 h. For instance, in the case of D-GO75, the dead cells were 78 ± 8% (1h), 92 ± 9% (2h) and 98 ± 3% (1h), 97 ± 5% (2h) for *E. coli* and *B. subtilis,* respectively (Fig. 8). This inactivation difference between these two different bacteria was previously reported for G, GO and PEI.[10, 35, 46]

While there are plenty of literature for the mechanisms of G and GO toxicity, the *h*-MoO_3, on the other hand, has not been extensively investigated for its antimicrobial activity.[10] In the dead/live assay, it was found that the antimicrobial activity of A-$MoO_3$50 was time dependent for both *E. coli* and *B. subtilis*. In addition, the incorporation of *h*-MoO_3 to an adhesive polymer (A-$MoO_3$50) resulted to coatings with antimicrobial activities comparable to other well-known antimicrobial materials used in this study (Fig. 8). These findings give a new option of selecting metal oxide nanoparticles (*h*-MoO_3) for antimicrobial applications.

Further examination of the microorganisms exposed to the coated surfaces was also done through SEM. The images showed damage of cell membranes, which led to cell death, after contact with coated surfaces (Fig. S7 and Fig. 9). The SEM images of samples incubated with the coated surfaces show that the cells had twisted shapes or were busted. In comparison, cells with smooth and healthy shapes were observed only on the control and uncoated slides. The images of the destroyed microorganisms were similar to graphene and graphene oxide cellular damage previously observed in other studies.[26] Similar results were also found for coatings with *h*-MoO_3 and PEI. These results suggest that the antimicrobial activity of the latter two materials involved cell membrane damage as well.

Further investigation of the antimicrobial property of the coated surfaces toward other Gram-negative and Gram-positive bacteria was also investigated, using *Pseudomonas aeruginosa*, *Streptococcus pyogenes* and *Staphylococcus epidermidis* cultures. The coated glass slides caused cell death upon contact with these microbes as well (Fig. S6). However, the highest inhibition activity was observed at longer incubation time (2h). This could be due to *P. aeruginosa*, *S. pyogenes* and *S. epidermidis* being more resistant microorganisms in general, since they are known to resist several antibiotics and drugs.[48-50] These results once again confirmed the effectivity of the adhesives for coating surfaces with antimicrobial materials.

Anti-biofilm effects of the coatings

Longer time exposure to investigate anti-biofilm formation was performed with the optimized coatings. During biofilm formation, there are a combination of different forces and interactions, such as van der Waals or electrostatic force and cell-substrate or cell-cell interaction on same surface.[51, 52] Previous studies have reported that PEI could also have anti-biofilm activity.[53] The results of this study confirmed that as coating component (in C-PEI75), PEI also exhibited anti-biofilm activity. The total biofilm of the coatings with PEI was 0.04 ± 0.01 and 0.01 ± 0.001 for *E. coli* and *B. subtilis* after 72 h growth, respectively (Fig. 10). Additionally, the total biomass of the biofilm after 72 h growth determined with the confocal microscope showed a reduced biomass compared to the control without the coating (Fig. S8). In the presence of antimicrobial coatings, the bacteria were inactivated upon contact with the antimicrobial surface, which led to a reduced biofilm growth. To further confirm these results, other

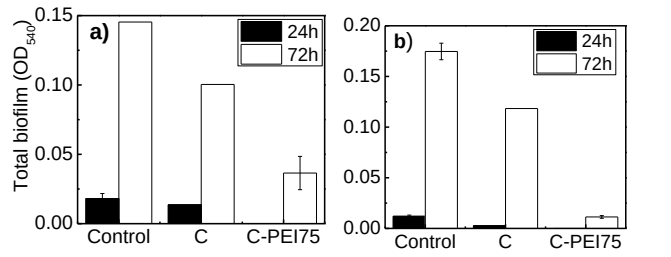

Fig. 10: The total *E. coli* (a) and *B. subtilis* (b) biofilm forming on surfaces containing adhesives and PEI 75% (C-PEI75) coatings.

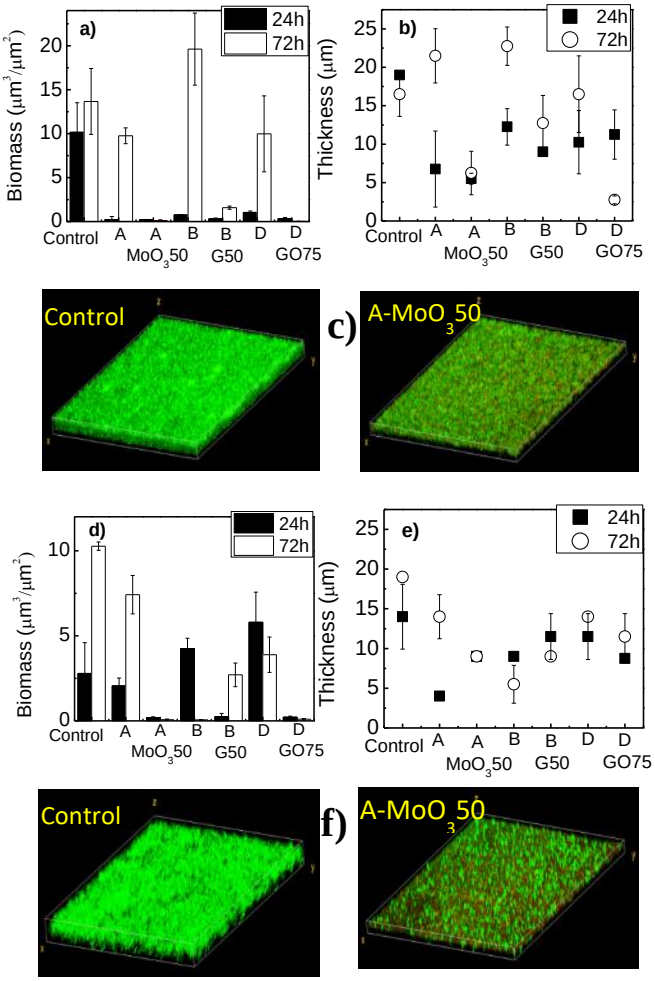

Fig. 11: (a) Biomass volume of *E. coli*, (b) biofilm thickness of *E. coli*, (c) images of *E. coli* with control and adhesive A with MoO_3 50%, (d) biomass volume of *B. subtilis*, (e) biofilm thickness of *B. subtilis* and (f) images of *B. subtilis* with control and adhesive A with MoO_3 50%. Column graphs (a and d) represents total biomass in 24h (solid black) and 72h (solid white). Point graph (b and e) correspond to the thickness of the biofilm in 24h (solid square black) and 72h (open circle). The control corresponds to glass slide without any coating.

microbes, such as *P. aeruginosa* and *S. pyogenes* were also tested for biofilm growth. Similar trends were observed, *i.e.* C-PEI75 coating prevented their biofilm formation (Fig S9).

In the case of the nanoparticles with the adhesives, all the coatings containing G, GO or *h*-MoO_3 also showed significant anti-biofilm activities. The biomass on the surface without any coating was 13.7 ± 3.7 μ^3/μ^2, while the presence of coating showed only 0.1 ± 0.08, 1.6 ± 0.2 and 0.02 ± 0.0 μ^3/μ^2 for A-$MoO_3$50, B-G50 and D-GO75, respectively, when exposed to *E. coli* for 72 h (Fig. 11). Significant anti-biofilm activity for other microorganisms, i.e. *P. aeruginosa* and *S. epidermidis*, was also observed with these coatings (Fig. S10).

It is worth pointing that the adhesives by themselves also inhibited, at some extend, biofilm growth. However, they did not present any antimicrobial property (Fig. 8 and 9). This biofilm inhibition could be because of the contact angle properties of the adhesives. It is known that the microbial adhesion and biofilm formation relies strongly on the hydrophobic and/or hydrophilic interactions of surfaces with microbial cells.[54]

Human toxicity of the coatings

In order to utilize the coatings for biomedical applications, these coatings were tested for cytotoxicity against the hTCEpi cell line. Results showed that no cell death was observed on surfaces with the new coatings (Fig. 12). These results confirmed that the composites of adhesives containing PEI, G, GO or *h*-MoO_3 are toxic against bacteria, but not to human cells. This implies safety and biocompatibility of these new coatings materials for use in bio-applications.

Mechanism of toxicity

Glutathione (GSH) is considered an important biological antioxidant. Depletion of GSH is proportional to the generation of ROS, such as hydrogen peroxide. Therefore, the reaction of GSH with ROS is often utilized as a direct measurement of oxidative stress in biological systems.[55] In biological systems, the glutathione peroxidase molecule reduces H_2O_2 into H_2O; while the GSH is oxidized into GSSG. The colorimetric reaction of GSH with 5,5'-dithiobis-(2-nitrobenzoic acid) DTNB (Ellman's reagent) can be used to determine the total loss of glutathione.[56] ROS has been determined to be one of the main mechanisms for nanomaterial toxicity. In a biological system, the cells can typically maintain the levels of ROS low to avoid damage of cellular components. Overproduction of ROS from external sources, such as nanomaterials can, however, create higher levels of oxidative stress that cannot be resolved by the cell defence mechanism system, which will result in cell damage.[57] Therefore, the ROS produced from antimicrobial agents (G, GO, MoO3 and PEI) will create excessive ROS, which will lead to cell death.

The antimicrobial materials (PEI, G, GO and *h*-MoO_3) were reported to interfere with the cell's oxidation repair mechanisms which was one of the factor contributing to cell death.[35, 58, 59] In this study, we also monitored the ROS production of the coating materials to gain insights about their mechanisms of action. The results showed that the incorporation of these antimicrobial materials in the adhesive polymers still express similar mechanisms of toxicity as their pristine counterparts as previously described in the literature.[35, 58, 59] All the coated slides produced a certain amount of ROS after 2 h contact with the GSH solution (Fig. 13). Although the ROS was produced by all coated slides, the graphene had the lowest ROS production, which could be due to the lack of oxygen functional groups present on graphene sheets. This phenomenon was previously reported in studies investigating different graphene based materials.[35] It is important to note that the glass slides coated with the adhesive polymer only (as negative control) did not produce ROS (Fig. 13).

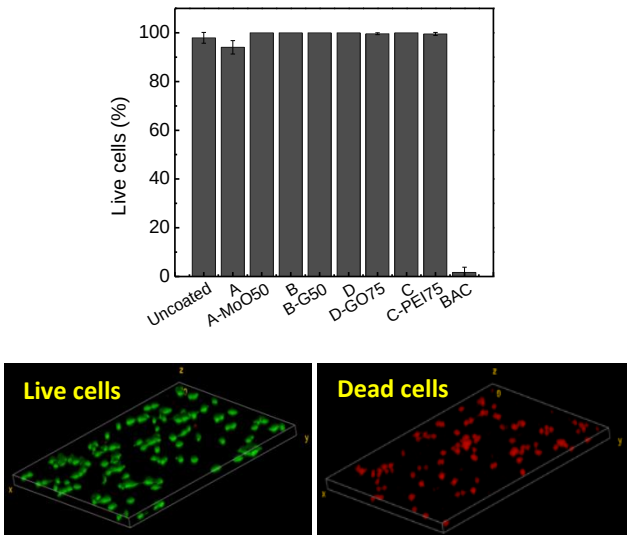

Fig. 12: Cytotoxicity of coated slides against the hTCEpi cell line (human corneal epithelial) expressed in terms of percentage of dead cells. The uncoated glass slide represents the negative control and BAC (benzalkonium chloride, 0.02%) represents positive control

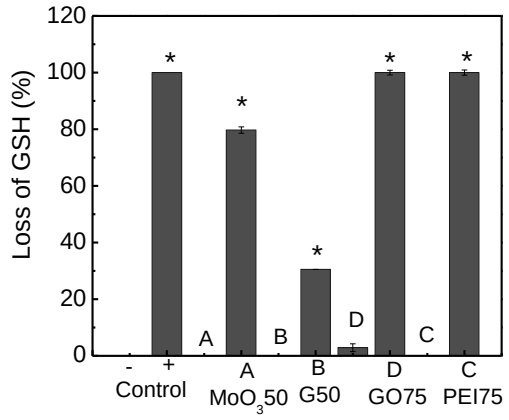

Fig. 13: Reactive oxygen species produced from the coatings. The results are expressed in terms of percentage of GSH loss in comparison to the negative control. The symbol (*) indicates the sample results are statistically different from the negative control.

Polymers are commonly used for biomedical applications, from natural polymers to synthetic polymers, such as poly(vinyl alcohol), polyethylene, polypropylene or poly(lactic acid), so it is not surprising the negligible production of ROS by the adhesives only.[60-62]

Conclusions

In the present study, several polymers with catechol side chains were successfully synthesized and blended with antimicrobial materials (PEI, G, GO, *h*-MoO_3) to generate antimicrobial and anti-biofilm coatings without presenting toxicity to human cells. The adhesive polymers were used as a component of the coating in amounts as low as 15% to immobilize the antimicrobial materials on the surface. The composites were also demonstrated to be stable under physiological conditions, and thus, could potentially be used in clinical and other biomedical applications to prevent growth of pathogenic bacteria on surfaces of medical devices. The results have also shown that the coating materials are active on a broad range of pathogenic microorganisms. Although our investigation was based on specific materials, it is possible to assume that the incorporation of PEI (and/or similar FDA approved polymer-based antimicrobials) in such formulations could potentially produce other types of coatings capable of preventing microbial attachment and biofilm formation.

Acknowledgements

The project was partially funded by the National Science Foundation awards#: 1130006 and 1150255. The authors would like to acknowledge Jay Harden (measurement of contact angles) and Marjorie Hernandez (Research Experience for Teachers, RET program) (preliminary results). The authors also would like to thank high school students: Mariam Khaldoon, Howard Yong and Akash Tarkunde for participating during the summer in the project.

References

1. C. R. Matos-Pérez, J. D. White and J. J. Wilker, *Journal of the American Chemical Society*, 2012, 134, 9498-9505.
2. H. Chung, P. Glass, J. M. Pothen, M. Sitti and N. R. Washburn, *Biomacromolecules*, 2010, 12, 342-347.
3. H. Lee, S. M. Dellatore, W. M. Miller and P. B. Messersmith, *Science*, 2007, 318, 426-430.
4. B. Zhang, Y. Chen, X. Zhuang, G. Liu, B. Yu, E.-T. Kang, J. Zhu and Y. Li, *Journal of Polymer Science: Part A: Polymer Chemistry*, 2010, 48, 2642-2649.
5. Z. Qin and M. J. Buehler, *Journal of the Mechanics and Physics of Solids*, 2014, 62, 19-30.
6. Y. Liu, K. Ai and L. Lu, *Chemical Reviews*, 2014, 114, 5057-5115.
7. J. Chen, H. Peng, X. Wang, F. Shao, Z. Yuan and H. Han, *Nanoscale*, 2014, 6, 1879-1889.
8. C. Zollfrank, K. Gutbrod, P. Wechsler and J. P. Guggenbichler, *Materials Science and Engineering: C*, 2012, 32, 47-54.
9. J. L. Fox, *Nat Biotech*, 2013, 31, 379-382.
10. K. A. Gibney, I. Sovadinova, A. I. Lopez, M. Urban, Z. Ridgway, G. A. Caputo and K. Kuroda, *Macromolecular Bioscience*, 2012, 12, 1279-1289.
11. B. Gao, X. Zhang and Y. Zhu, *Journal of Biomaterials Science, Polymer Edition*, 2007, 18, 531-544.
12. K. N. Stevens, S. Croes, R. S. Boersma, E. E. Stobberingh, C. van der Marel, F. H. van der Veen, M. L. Knetsch and L. H. Koole, *Biomaterials*, 2011, 32, 1264-1269.
13. I. E. M. Carpio, C. M. Santos, X. Wei and D. F. Rodrigues, *Nanoscale*, 2012, 4, 4746-4756.
14. C. M. Santos, J. Mangadlao, F. Ahmed, A. Leon, R. C. Advincula and D. F. Rodrigues, *Nanotechnology*, 2012, 23, 395101.
15. Z. Liu, J. T. Robinson, X. M. Sun and H. J. Dai, *Journal of the American Chemical Society*, 2008, 130, 10876-+.

16. X. M. Sun, Z. Liu, K. Welsher, J. T. Robinson, A. Goodwin, S. Zaric and H. J. Dai, *Nano Research*, 2008, 1, 203-212.
17. C. M. Santos, M. C. Tria, R. A. Vergara, F. Ahmed, R. C. Advincula and D. F. Rodrigues, *Chem Commun (Camb)*, 2011, DOI: 10.1039/c1cc11877c.
18. E. Comini, L. Yubao, Y. Brando and G. Sberveglieri, *Chemical Physics Letters*, 2005, 407, 368-371.
19. N. Desai, S. Mali, V. Kondalkar, R. Mane, C. Hong and P. Bhosale, *Journal of Nanomedicine & Nanotechnology*, 2015, 2015.
20. K. Karthikeyan, P. Mariappan, V. Murugan and K. Sang Jae, *Nanotechnology*, 2014, 25, 315101.
21. A. Chithambararaj, N. S. Sanjini, S. Velmathi and A. Chandra Bose, *Physical Chemistry Chemical Physics*, 2013, 15, 14761-14769.
22. H. N. Nguyen, S. Castro and D. F. Rodrigues, *Environmental Science: Nano*, 2017.
23. H. Han, J. Wu, C. W. Avery, M. Mizutani, X. Jiang, M. Kamigaito, Z. Chen, C. Xi and K. Kuroda, *Langmuir*, 2011, 27, 4010-4019.
24. Y. Yuan and T. R. Lee, in *Surface Science Techniques*, eds. G. Bracco and B. Holst, Springer Berlin Heidelberg, Berlin, Heidelberg, 2013, DOI: 10.1007/978-3-642-34243-1_1, pp. 3-34.
25. C. A. Schneider, W. S. Rasband and K. W. Eliceiri, *Nature methods*, 2012, 9, 671-675.
26. I. E. Mejias Carpio, C. M. Santos, X. Wei and D. F. Rodrigues, *Nanoscale*, 2012, 4, 4746-4756.
27. J. Peña-Bahamonde, V. San Miguel, H. N. Nguyen, R. Ozisik, D. F. Rodrigues and J. C. Cabanelas, *Carbon*, 2017, 111, 258-268.
28. L. A. Pratt and R. Kolter, *Mol Microbiol*, 1998, 30, 285-293.
29. D. F. Rodrigues and M. Elimelech, *Environmental Science & Technology*, 2010, 44, 4583-4589.
30. A. Heydorn, A. T. Nielsen, M. Hentzer, C. Sternberg, M. Givskov, B. K. Ersbøll and S. Molin, *Microbiology*, 2000, 146, 2395-2407.
31. D. F. Rodrigues and M. Elimelech, *Biofouling*, 2009, 25, 401-411.
32. D. F. Rodrigues and M. Elimelech, *Environ Sci Technol*, 2010, 44, 4583-4589.
33. J. Kim, B. Wu, S. M. Niedzielski, M. T. Hill, R. M. Coleman, A. Ono and A. Shikanov, *Journal of biomedical materials research. Part A*, 2015, 103, 2701-2710.
34. G. L. Ellman, *Archives of Biochemistry and Biophysics*, 1959, 82, 70-77.
35. S. Liu, T. H. Zeng, M. Hofmann, E. Burcombe, J. Wei, R. Jiang, J. Kong and Y. Chen, *ACS Nano*, 2011, 5, 6971-6980.
36. Q. Lin, D. Gourdon, C. Sun, N. Holten-Andersen, T. H. Anderson, J. H. Waite and J. N. Israelachvili, *Proceedings of the National Academy of Sciences*, 2007, 104, 3782-3786.
37. H. Lee, B. P. Lee and P. B. Messersmith, *Nature*, 2007, 448, 338-341.
38. F. Chauvin, A. M. Alb, D. Bertin, P. Tordo and W. F. Reed, *Macromol Chem Phys*, 2002, 203, 2029-2041.
39. D. S. S. M. Uppu, S. Samaddar, J. Hoque, M. M. Konai, P. Krishnamoorthy, B. R. Shome and J. Haldar, *Biomacromolecules*, 2016, 17, 3094-3102.
40. K. Kuroda, G. A. Caputo and W. F. DeGrado, *Chemistry (Weinheim an der Bergstrasse, Germany)*, 2009, 15, 10.1002/chem.200801523.
41. Z. Liu, Z. Zhang, C. Zhou and Y. Jiao, *Progress in Polymer Science*, 2010, 35, 1144-1162.
42. H. Takahashi, E. F. Palermo, K. Yasuhara, G. A. Caputo and K. Kuroda, *Macromolecular Bioscience*, 2013, 13, 1285-1299.
43. E. F. Palermo, I. Sovadinova and K. Kuroda, *Biomacromolecules*, 2009, 10, 3098-3107.
44. A. Jarosz, M. Skoda, I. Dudek and D. Szukiewicz, *Oxidative Medicine and Cellular Longevity*, 2016, 2016, 5851035.
45. F. Taherian, V. Marcon, N. F. A. van der Vegt and F. Leroy, *Langmuir*, 2013, 29, 1457-1465.
46. I. E. M. Carpio, J. D. Mangadlao, H. N. Nguyen, R. C. Advincula and D. F. Rodrigues, *Carbon*, 2014, 77, 289-301.
47. N. Dighore, S. Jadhav, P. Anandgaonker, S. Gaikwad and A. Rajbhoj, *Journal of Cluster Science*, 2016, 1-10.
48. E. B. Hirsch and V. H. Tam, *Expert review of pharmacoeconomics & outcomes research*, 2010, 10, 441-451.
49. S. S. Y. Wong and K.-Y. Yuen, *Emerg Microbes Infect*, 2012, 1, e2.
50. M. Otto, *Nature reviews. Microbiology*, 2009, 7, 555-567.
51. D. Saeki, Y. Nagashima, I. Sawada and H. Matsuyama, *Colloids and Surfaces A: Physicochemical and Engineering Aspects*, 2016, 506, 622-628.
52. R. M. Donlan, *Emerging Infectious Diseases*, 2002, 8, 881-890.
53. J. Barros, A. Dias, M. Rodrigues, C. Pina-Vaz, M. Lopes and I. Pina-Vaz, *The journal of contemporary dental practice*, 2015, 16, 427-432.
54. Y. Liu, S.-F. Yang, Y. Li, H. Xu, L. Qin and J.-H. Tay, *Journal of Biotechnology*, 2004, 110, 251-256.
55. S. Gurunathan, J. W. Han, A. A. Dayem, V. Eppakayala and J.-H. Kim, *International journal of nanomedicine*, 2012, 7, 5901-5914.
56. K. Apel and H. Hirt, *Annu. Rev. Plant Biol.*, 2004, 55, 373-399.
57. V. J. Thannickal and B. L. Fanburg, *American Journal of Physiology-Lung Cellular and Molecular Physiology*, 2000, 279, L1005-L1028.
58. K. Krishnamoorthy, M. Veerapandian, K. Yun and S. J. Kim, *Colloids and surfaces. B, Biointerfaces*, 2013, 112, 521-524.
59. A. Hall, L. Parhamifar, M. K. Lange, K. D. Meyle, M. Sanderhoff, H. Andersen, M. Roursgaard, A. K. Larsen, P. B. Jensen, C. Christensen, J. Bartek and S. M. Moghimi, *Biochimica et Biophysica Acta (BBA) - Bioenergetics*, 2015, 1847, 328-342.
60. A. Gautam and S. Ram, *Materials Chemistry and Physics*, 2010, 119, 266-271.
61. E. Seyedjafari, M. Soleimani, N. Ghaemi and I. Shabani, *Biomacromolecules*, 2010, 11, 3118-3125.
62. P. A. Zapata, L. Tamayo, M. Páez, E. Cerda, I. Azócar and F. M. Rabagliati, *European Polymer Journal*, 2011, 47, 1541-1549.

